High Current Integrated Microinductors and Microtransformers using Low Temperature Fabrication Processes

Jae Y. Park* and Mark G. Allen
School of Electrical and Computer Engineering
Georgia Institute of Technology
Atlanta, GA 30332-0269
*Office: 404-894-9907, Fax: 404-894-5028, E-mail: gt1216a@prism.gatech.edu

Abstract

In many systems which utilize magnetic components, e.g., miniaturized DC-DC converters, PCMCIA cards, and modem standoff transformers, the magnetic device is the largest single component in the package. Surface-mount magnetic devices may be unacceptably thick where low profiles are required. Our approach to this problem is to use micromachining techniques to realize inductors and transformers built into the multilayer structure of a multi-chip package, allowing compact integration with chips, sensors, and other components. Microinductors and microtransformers composed of thick cores and multiwinding conductors have high inductance, high saturation current, and low resistance compared with previous integrated inductors. The total size of the microinductive device is 4 mm x 4 mm x 0.145 mm having 156 turns of multilevel electroplated copper coils (40 μm thick) and electroplated permalloy magnetic core (35 μm thick). These devices have inductances up to 1.5 μH and current-carrying capability of up to 3A steady DC current, making them applicable to power converters. The processing steps chosen are all low-temperature, which allows the use of low cost substrates such as MCM-L compatible materials.

Key words: microinductor, microtransformer, low temperature, inductance, saturation current, Q-factor

Introduction

Microinductors and microtransformers which have high values of inductance, Q-factor, coupling factor, and saturation current are useful in many applications such as microsensors, microfilters, and miniaturized switched power convereters integrated with multichip modules or electronic systems [1-2]. In particular, the use of these devices is necessary to miniaturize DC/DC converters used as power supplies in communications, military/aerospace applications, and computer/peripheral or other portable devices. Miniaturized DC/DC converters using microinductors and microtransformers have many potential advantages such as high frequency operation, efficiency, quality, low cost, and low power loss [3-7]. Our approach is to fabricate these required inductive components using low-temperature micromachining techniques and low-cost MCM-L compatible substrates in order to enable low-cost, fully integrated versions of these power converter devices.

Design and Modeling

Figure 1 shows a conceptual view of microinductors and microtransformers which are composed of a magnetic core and multilevel metal conductors. The microinductive component is designed to have a completely closed magnetic circuit to minimize leakage flux, since leakage flux does not contribute to the total inductance of the device and can cause interference with other integrated circuitry on the same substrate. An airgap is optionally included in the magnetic core to desensitize to applied field and increase the saturation current. Electroplating techniques are used to fabricate the conductor lines and the vias, as electroplated metal contacts usually have a relatively low metal contact resistance.

(a) Pattern of microinductor

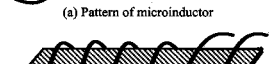

(b) Pattern of microtransformer

Figure 1. Schematic patterns of microinductors and microtransformers

The Reluctance $\mathcal{R}$ and inductance L are calculated by the following equation:

$$\mathfrak{R} = \frac{\ell_c}{\mu_0 \mu_r A_c} \qquad (1)$$

$$L = \frac{\mu_0 \mu_r A_c N^2}{\ell_c} = \frac{N^2}{\Re} \qquad (2)$$

where A_c is the cross-sectional area of the film magnetic core, ℓ_c is the length of the closed magnetic core, N is the number of coil turns, and μ_0 and μ_r are the permeability of the vacuum and the relative permeability of the magnetic core, respectively. The quality factor and dc resistance can be defined as:

$$Q = \frac{\omega L}{R}, \; R = \rho \frac{\ell_w}{A_w} \qquad (3)$$

where Aw is the cross-sectional area of the conductor, ω is the radian frequency, ℓ_w is the length of the conductor lines, and ρ is the resistivity of the conductor material. From the above equations (2) and (3), it is seen that inductance and Q-factor are linearly proportional to μ_r and A_c in the microinductive components. But the inductance is not proportional to the square of coil turns in the components, since due to fabrication constraints on the microinductive component, larger numbers of coil turns require a longer core length. The important parameter, coupling factor, in microtransformers is calculated by:

$$K = \frac{L_m}{\sqrt{L_p L_s}}, L_m = \frac{\mu_0 \mu_r A_c N_p N_s}{\ell_c} \qquad (4)$$

where L_m is the mutual inductance, Lp is the primary inductance, and L_s is the secondary inductance in microtransformers.

$$\Phi = BA_c = \frac{NI}{\Re} \Rightarrow I_{sat} = \frac{B_{sat} \Re A_c}{N} \qquad (5)$$

Equation (5) shows that the DC saturation current is proportional to the saturation flux density. Permalloy (80% nickel-20% iron) which has a saturation flux density of approximately 0.9T is used as core material to demonstrate the geometry of microinductors and microtransformers. Eddy current losses in the magnetic core as well as the skin depth effect in the conductor are neglected in these calculations.

Fabrication

Among several obstacles encountered in fabricating microinductors and microtransformers, the major difficulty comes from the fabrication of thick wrapping coils which have a low conductor resistance. Thick molds for the wrapping coils are patterned using thick photoresist and photolithography. Electroplating is a favorable technique for deposition of thick metal conductors, but electroplating usually requires a plating seed layer which must be removed after completing the fabrication structure. Consequently, the seed layer used for lower conductor lines should serve as the plating seed layer for the via and remain until the fabrication is completed. At this time, the seed layer must be removed or all of the coils will be shorted. Unfortunately, the seed layer is now difficult to remove, as it is at the bottom of the structure. Simple blanket etching to expose the seed layer will not work as the magnetic core placed on the top of the lower conductor lines as a mask to prevent complete exposure of the seed layer. To solve this problem, a mesh-type seed layer is used. This mesh-type seed layer can serve as the electroplating seed layer for the lower conductor lines and vias until the fabrication is completed. When the fabrication of these devices is completed, the edges of the mesh-type seed layer can be exposed using plasma etch and then removed, ensuring the electrical isolation of the coils. Another difficulty in the fabrication comes from the need to fabricate a thick magnetic core (for low magnetic reluctance) which should be placed on the top of the insulated lower conductor lines. The relatively high aspect ratio of the magnetic core causes a serious difficulty in patterning the vias and the upper conductor lines, due to poor planarization of the surface. Another seed layer which has the same shape as magnetic core is used to solve these problems.

Figure 2 shows a brief fabrication process of these devices. The process started with a glass as low cost substrate. Chromium/copper/chromium layers were deposited to form an seed layer for electroplating using electron-beam evaporation. This mesh-type seed was patterned to form a conductor network to be removed after serving as the seed layer for plating of the conductor and vias. Polyimide (Dupont PI2611) was spun on the top of mesh-type seed layer to construct electroplating molds for the bottom conductor lines. Four coats were made to obtain 40 μm thick polyimide molds. After coating, the polyimide was cured at 300 °C for 1 hour in nitrogen. An aluminum layer (0.2 μm thick) was deposited on top of the cured polyimide as a hard mask for dry etching. Molds for lower conductor lines were patterned and etched using an plasma etcher until the seed layer was exposed. After etching the aluminum hard mask and the top chromium of the seed layer, the molds were filled with electroplated copper using standard electroplating techniques.

One coat of polyimide was cast to isolate the lower conduetor lines and the magnetic core. The seed layer was deposited, patterned in mesh-type, coated with polyimide (35 μm thick), and hard-cured. An aluminum layer (0.2 μm thick) was deposited as a

hard mask for dry etching. A mold for the magnetic core was patterned and etched until the seed layer was exposed. After etching the aluminum hard mask and the top chromium of the seed layer, the mold was filled with plated nickel-iron using standard electroplating techniques.

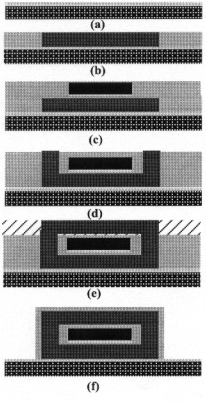

Figure 2. Fabrication procedure for microinductors and microtransformers: (a) patterning of mesh seed layer; (b) electroplating of lower conductors and passivation; (c) patterning of mesh seed layer and electroplating of magnetic core; (d) via conductor plating; (e) upper conductor plating; (f) removal of polyimide and mesh seed layer

One coat of polyimide was spin-cast and cured to insulate the core and upper conductor lines. Via holes were patterned on a sputtered aluminum and etched through the polyimide layer using 100% oxygen plasma. Vias were filled with electroplated copper. A copper/chromium seed layer was deposited, and molds for the upper conductor lines were formed using thick photoresist. The molds were filled with plated copper and removed. After removing the seed layer, a polyimide passivation layer coated and cured to protect the top conductor lines. The polyimide was optionally masked and etched to the bottom. The bottom mesh seed layer was then wet etched. At the completion of fabrication, samples were diced and tested.

Figures 3 and 4 show microinductors and microtransformers which consist of electroplated copper conductor lines (40 μm thick), electroplated magnetic core (35 μm), and polyimide PI-2611 as an insulation material. Figures 5 and 6 show scanning electron micrograph top views of microinductors and microtransformers taken after removing the polyimide. Figures 7 and 8 show side view, wrapped conductors, a magnetic core, lower and upper conductors, and via interconnections of microinductor.

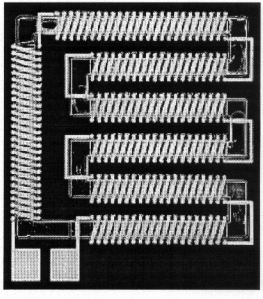

Figure 3. Photomicrograph of microinductor with air gap

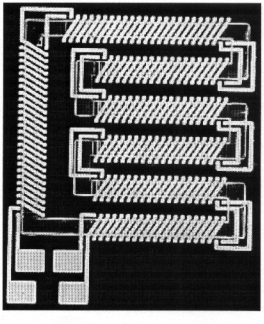

Figure 4. Photomicrograph of microtransformer with no air gap

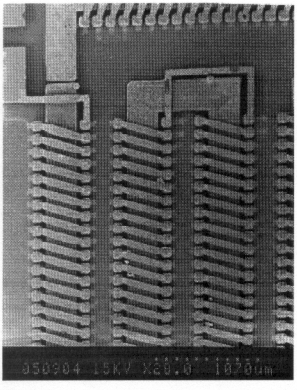

Figure 5. Scanning electron micrograph of the top view of microinductor with air gap

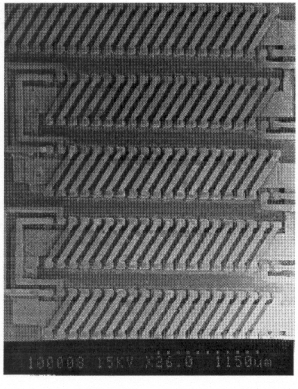

Figure 6. Scanning electron micrograph of the top view of microtransformer

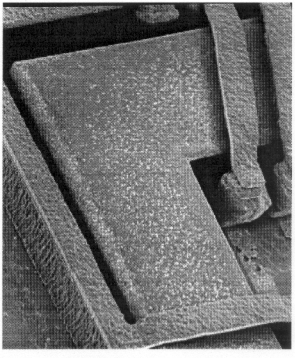

Figure 7. Scanning electron micrograph of the side view of microinductor

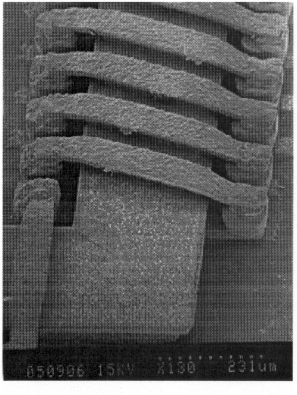

Figure 8. Scanning electron micrograph of wrapped conductors, vias, and a magnetic core of microinductor

Experimental Results and Analysis

Prior to measurement of components, an electroplated core test sample was characterized using a vibrating sample magnetometer. The test sample shows a saturation flux density of 0.9 T and a relative permeability of 600 as shown in Figure 9. Once the characteristics of the test sample were determined characteristics of actual fabricated components were measured. Inductance, resistance, Q-factor, and gain of fabricated inductive components were measured by a Hewlett-Packard impedance/gain-phase analyzer 4194A. Figure 10 shows that at low frequencies, the microinductor with no airgap has slightly higher inductance than the microinductor with airgap as expected, since the core with no airgap has a lower reluctance than the core with airgap. At higher frequencies, the resistance of the microinductor with airgap is lower than that of the one with no airgap as shown in Figure 11, which could be an indication of lower iron loss in the airgap device. Figure 12 shows that the microinductor with airgap has a higher Q-factor (3.1 at 40 MHz) than the no airgap device (2.5 at 40 MHz).

DC saturation current was measured using a Wayne kerr 3245 precision inductance analyzer. DC saturation current is generally defined as the current at which the inductance value falls off 20 % of the measured inductance without the applied DC current (the 20% falloff current is defined as I_{80}). Figure 13 shows that the microinductor with air gap has much higher saturation current (I_{80} = 250 mA) than the no airgap device (I_{80} = 85 mA). Finally, a fully integrated microtransformer with primary to secondary winding ratio of 1:1 has 2 dB loss when operating at 15 MHz as shown in Figure 14.

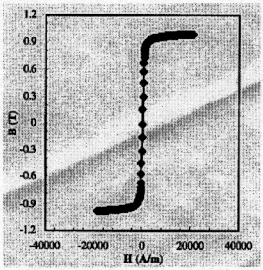

Figure 9. B-H characteristic of fabricated permalloy core test sample

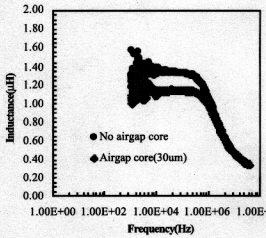

Figure 10. Comparison of the inductance of microinductors

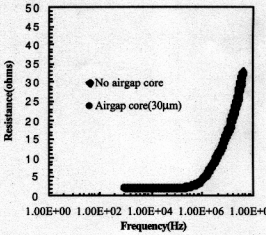

Figure 11. Comparison of the resistance of microinductors

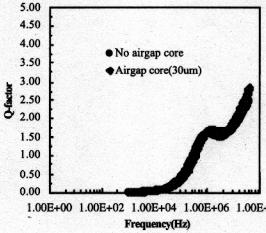

Figure 12. Comparison of the Quality factor of microinductors

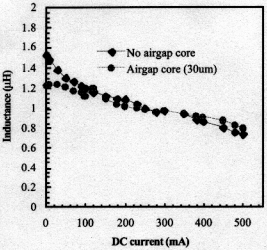

Figure 13. Comparison of the saturation current of microinductors

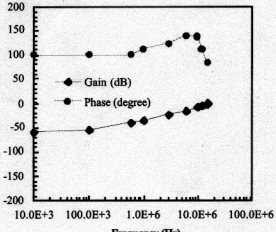

Figure 14. Gain and phase analysis of microtransformer with no air gap

Conclusions

Fully integrated microinductors and microtransformers have been fabricated on glass using micromachining and multilevel metallization techniques. Only low temperature processes have been used in fabrication, and the fabrication sequences are packaging-compatible. By comparing microinductors with airgaps in the core to devices without airgaps in the core, it has been shown that airgap core devices exhibit improved characteristics. These microinductors and microtransfomers have potential application as integrated passives for multichip modules, microfilters, miniaturized DC/DC power converters, and micromagnetic sensors and actuators.

Acknowledgment

This research was supported by the National Science Foundation through the Georgia Tech/NSF Engineering Research Center in Electronic Packaging (contract EEC-9402723). Microfabrication was carried out at the Microelectronics Research Center of Georgia Tech. Assistance with measurement of magnetic property of permalloy thin film from Mr. William Taylor of Georgia Tech as well as Mr. Michael Schneider and Professor Henry Baltes of the Swiss Federal Institute of Technology (ETH-Zürich) are gratefully acknowledged.

References

[1] Jae Y. Park and Mark G. Allen, "A comparison of micromachined inductors with different magnetic core materials", *IEEE 46th Electronic Components & Technology Conference*, Orlando, Fl, pp. 375~381, 1996

[2] C. H. Ahn, Y. J. Kim, and Mark G. Allen, "A fully integrated planar toroidal with a micromachined Ni-Fe magnetic bar", *IEEE Transactions on Components, Hybrids and manufacturing Technology*, 1993

[3] H. M. Greenhouse, "Design of planar rectangular microelectronic inductors", *IEEE Transactions Parts, Hybrids, and Packaging*, vol. PHP-10, no.2, pp.101~109,1974

[4] O. Oshiro, H. Tsujimoto, and K. Shirae, "A novel miniature planar inductor", *IEEE Transactions on Magnetics*, vol. 23, no.2, pp. 3759 ~3761, 1987

[5] M. Yamaguchi, M. Matsumoto, H. Ohzeki, and K. I. Arai, "Fabrication and basic characteristics of dry-etched microinductors", *IEEE Transactions on Magnetics*, vol. 26, pp. 2014~2016, 1990

[6] K. Yamasawa, K. Maruyama, I. Hirohama, and P. Biringer, "High frequency operation of aplanar-type microtransformer and its application to multi layered switching regulators", *IEEE Transactions on Magnetics*, vol. 26, no.3, pp. 1204 ~1209, 1990

[7] K. Yamaguchi, S. Ohnuma, H. Matsuki, and K. Murakami, "Characteristics of a thin film microtransformer with circular spiral coils", *IEEE Transactions on Magnetics*, vol. 29, no.5, pp. 2232 ~2237, 1993